

AD-755 392

FURTHER EXPERIMENTAL STUDIES ON BUCKLING  
OF INTEGRALLY RING-STIFFENED CYLINDRICAL  
SHELLS UNDER AXIAL COMPRESSION

Tanchum Weller, et al

Technion - Israel Institute of Technology  
Haifa, Israel

April 1972

DISTRIBUTED BY:

**NTIS**

National Technical Information Service  
U. S. DEPARTMENT OF COMMERCE  
5285 Port Royal Road, Springfield Va. 22151

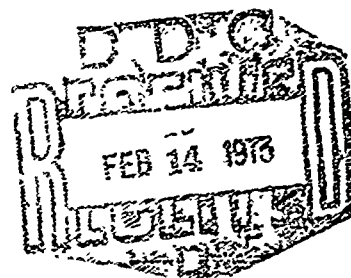
AD 755392

SCIENTIFIC REPORT No. 6

**FURTHER EXPERIMENTAL STUDIES ON BUCKLING OF  
INTEGRALLY RING-STIFFENED CYLINDRICAL SHELLS  
UNDER AXIAL COMPRESSION**

BY

TANCHUM WELLER  
JOSEF SINGER



Department of Aeronautical Engineering,  
Technion — Israel Institute of Technology  
Haifa, Israel

T. A. E. REPORT No. 138

NATIONAL TECHNICAL  
INFORMATION SERVICE

Approved for public release;  
distribution unlimited.

R3d

ADDITION OF	
NTS	Write Section <input checked="" type="checkbox"/>
DT	Write Section <input type="checkbox"/>
DT	Write Section <input type="checkbox"/>
BY	
DISTRIBUTION/AVAILABILITY CODES	
Dist.	Publ. 249/47 SPECIAL
A	

This document has been approved for public release and sale, its distribution is unlimited.

Qualified requestors may obtain additional copies from the Defense Documentation Center, all others should apply to the Clearinghouse for Federal Scientific and Technical Information.

UNCLASSIFIED

Security Classification

## DOCUMENT CONTROL DATA - R &amp; D

(Security classification of title, body of abstract and indexing annotation must be entered when the overall report is classified)

1. ORIGINATING ACTIVITY (Corporate author) TECHNION RESEARCH AND DEVELOPMENT FOUNDATION DEPARTMENT OF AERONAUTICAL ENGINEERING HAIFA, ISRAEL		2a. REPORT SECURITY CLASSIFICATION UNCLASSIFIED	
		2b. GROUP	
3. REPORT TITLE FURTHER EXPERIMENTAL STUDIES ON BUCKLING OF INTEGRALLY RING-STIFFENED CYLINDRICAL SHELLS UNDER AXIAL COMPRESSION			
4. DESCRIPTIVE NOTES (Type of report and inclusive dates) Scientific Interim			
5. AUTHOR(S) (First name, middle initial, last name) TANCHUM WELLER JOSEF SINGER			
6. REPORT DATE Apr 1972		7a. TOTAL NO. OF PAGES 38	7b. NO. OF REFS 16
8a. CONTRACT OR GRANT NO. F61052-69-C-0040		9a. ORIGINATOR'S REPORT NUMBER(S) T.A.E. Report No, 138 Scientific Report No. 6	
b. PROJECT NO. 9782-02			
c. 61102F		9b. OTHER REPORT NO(S) (Any other numbers that may be assigned this report) AFOSR - TR - 78 - 0119	
d. 681307			
10. DISTRIBUTION STATEMENT Approved for public release; distribution unlimited.			
11. SUPPLEMENTARY NOTES TECH, OTHER		12. SPONSORING MILITARY ACTIVITY AF Office of Scientific Research (NAM) 1400 Wilson Blvd. Arlington, Va. 22209	
13. ABSTRACT An experimental study of the buckling of closely spaced integrally stiffened cylindrical shells under axial compression was carried out to determine the influence of shell and ring geometry on the applicability of linear theory. 29 specimens fabricated from 7075-T6 aluminium alloy with different geometries were tested. Test specimens were designed to fail in general instability and under low critical stresses to assure elastic buckling. Agreement of experimental results of the present study, and of those obtained in other studies with linear theory was found to be governed primarily by the ring area parameter, $(A_2/ah)$ . Values of linearity, $p$ , (ratio of experimental buckling load to the predicted one) higher than 80% were obtained for $(A_2/ah) - 0.3$ and a clear trend towards $p=1$ was observed with increasing values of this parameter. Correlation with lineary theory was also found to be influenced by ring spacing, $(a/h)$ , or rather the combination $(a/h) (1 + (A_2/ah))^{-1/2}$ . No significant effect of shell and other ring parameters on the correlation with linear theory could be discerned for the shells tested. By a conservative structural efficiency criterion it was observed that only for low values of the area parameter, $(A_2/ah) - 0.5$ ring-stiffened shells are more efficient than equivalent weight isotropic ones. Highest efficiencies are obtained for $(A_2/ah) - 0.2$ .			

D FORM 1473  
1 NOV 65

UNCLASSIFIED

UNCLASSIFIED

Security Classification

14. KEY WORDS	LINK A		LINK B		LINK C	
	ROLE	WT	ROLE	WT	ROLE	WT
RING STIFFENED SHELLS EXPERIMENTAL STUDY OF BUCKLING CORRELATION WITH LINEAR THEORY INFLUENCE OF RING GEOMETRY STRUCTURAL EFFICIENCY						

IIa

UNCLASSIFIED

Security Classification

APRIL 1972

SR-6

SCIENTIFIC REPORT NO. 6

FURTHER EXPERIMENTAL STUDIES ON BUCKLING OF  
INTEGRALLY RING-STIFFENED CYLINDRICAL SHELLS  
UNDER AXIAL COMPRESSION

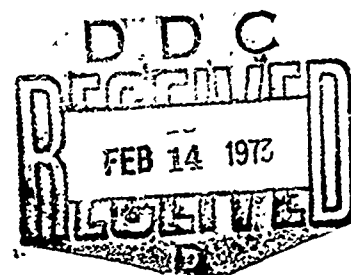
by

TANCHUM WELLER

JOSEF SINGER

Department of Aeronautical Engineering  
Technion - Israel Institute of Technology  
Haifa, Israel

T.A.E. REPORT No. 138



The research reported in this document has been sponsored by the Air Force Office of Scientific Research, through the European Office of Aerospace Research, United States Air Force under Contract F61052-69-C-0040.

IIb

## LIST OF CONTENTS

	<u>PAGE NO.</u>
ABSTRACT	I
LIST OF SYMBOLS	II - III
LIST OF FIGURES	IV
1. INTRODUCTION	1 - 3
2. TEST SET-UP AND PROCEDURE	4 - 5
3. TEST SPECIMENS	6 - 7
4. EXPERIMENTAL RESULTS AND DISCUSSION	8 - 13
ACKNOWLEDGEMENT	14
REFERENCES	15 - 17
TABLE 1	18 - 19
TABLE 2	20 - 21

IIc

LIST OF SYMBOLS

$A_2$	cross sectional area of rings
$a$	distance between rings for a cylindrical shell (see Fig. 1).
$c, d$	the width and height of rings (see Fig. 1).
$D$	$Eh^3/12(1 - \nu^2)$ .
$e_2$	eccentricity of rings (see Fig. 1).
$E$	modulus of elasticity.
$G$	shear modulus.
$h$	thickness of shell.
$I_{22}$	moment of inertia of ring cross-section about its centroidal axis.
$I_{t2}$	torsional constant of stiffener cross section.
$K, n$	material constants.
$L$	length of shell between bulkheads.
$M_x$	moment resultant acting on element.
$N_x, N_{x\phi}$	membrane force resultants acting on element.
$N$	number of rings.
$n$	number of half axial waves in cylindrical shell.
$P_{cl}$	classical buckling load for isotropic cylinder for "classical simple supports (SS3)
$(P_{cr})_{App}$	$= P_{cl}[1 + (A_2/ah)]^{1/2}$ approximate critical load.
$(P_{cr})_{SS3}$	linear theory general instability for stiffened cylinder with "smeared" stiffeners.



$P_{exp}$	experimental buckling load	
$(P_{LOC})_{SS3;SS4}$	critical local buckling loads corresponding to SS3 and SS4 boundary conditions, respectively.	
$(P_{LOC})_{spring}$	critical local buckling load corrected for springs (Eq. 7 of [1]).	
$Q$	$= [2.85 (1-\nu^2)^{-1/2} (R/h)]^{1/2}$	safe ring spacings
$R$	radius of cylindrical shell (see Fig. 1).	
$t$	number of circumferential waves.	
$t_{exp}$	experimental number of circumferential waves	
$u, v, w$	non-dimensional displacements, $u = (u^*/R), v = (v^*/R), w = (w^*/R)$ (see Fig. 1).	
$x^*, z^*, \phi$	axial coordinate along a generator, radial and circumferential coordinates (see Fig. 1).	
$Z$	$= (1 - \nu^2)^{1/2} (L/R)^2 (R/h)$	Batdorf shell parameter.
$\epsilon_x, \epsilon_\phi$	middle surface strains	
$\eta_{t2}$	$G_2 I_{t2} / aD$	
$\eta$	structural efficiency	
$\lambda$	$= (PR/\pi D)$	axial compression parameter for cylindrical shell.
$\nu$	Poisson's ratio	
$\rho$	"linearity" $= P_{exp}/P_{cr}$	
$\sigma_{y 0.1\%}$	stress at 0.1% of strain.	
$\sigma_{cr}$	critical stress	
SS3	simple supports	$v = N_x = w = M_x = 0$
SS4	simple supports	$u = v = w = M_x = 0$

LIST OF FIGURES

Fig. No.

1. Notations
2. Test Set - up
3. "Linearity" of Ring-Stiffened Shells as a Function of Ring Area Parameter,  $(A_2/ah)$ .
4. "Linearity" of Ring-Stiffened Shells as a Function of Ring Spacing,  $(a/h)$
5. "Linearity" of Ring-Stiffened Shells as a Function of  $(a/h) [1+(A_2/ah)]^{-1/2}$
6. Structural Efficiency of Ring-Stiffened Shells.
7. Typical Post Buckling Patterns
8. Growth of Surface Deflections At Stages of Loading Very Close to Buckling (Shell AR-14a).

## 1. INTRODUCTION

In references [1] and [2] the buckling under axial compression of closely spaced integrally ring-stiffened circular cylindrical shells, was studied experimentally, and the influence of stiffener and shell geometry on the applicability on classical linear theory was investigated. The shells of [1] and [2] were fabricated from two steel alloys with noticeably different mechanical properties (see Fig. 8 of [3]). The specimens differed in nominal dimensions, and represented shells with different  $R/h$  ratios. The experimental results of [1] and [2] were correlated with the predicted "classical" linear buckling loads, corresponding to  $SS3(N_x = v = 0)$  simply supported boundary conditions (see [4] & [5]) and with the results of other experimental investigations, [6] to [8]. The correlation with linear theory was shown there to be primarily affected by the ring-area parameter ( $A_2/ah$ ). For  $A_2/ah > .15$  values of "linearity" (ratio of experimental buckling load to the predicted one) above 70 % were achieved.

The present tests with specimens made of 7075-T6 aluminium alloy are a continuation of the earlier studies of [1] and [2] and aim at a better definition of the effect of stiffener geometry on the adequacy of linear theory. These tests are especially concerned with the range of low values of the ring-area parameter,  $A_2/ah < 0.2$  for which the predictions of linear theory were found to be unsatisfactory in [1] and [2]. The few earlier results in this range exhibited noticeable scatter. Hence, the present tests were carried out in order to verify the results of [1] and [2] and to establish a lower bound for applicability of linear theory.

As in earlier tests, care was taken in the present study to load the shells through their mid skin in order to avoid load eccentricity effects (see Fig. 4 of [1] and [9] to [13]).

Local buckling of the sub-shells between rings may also be the cause of low values of "linearity". This mode of failure was discussed in [1]. The discussion of [1] deals only with short unstiffened shells with either "classical" SS3 simple supports boundary conditions or elastic supports with zero axial restraint. The end conditions of the sub-shells are, however, closer to the SS4( $u = v = 0$ ) boundary condition and hence for local buckling this type of boundary conditions should be considered.

The general instability of the stiffened shells was again calculated with "smeared"stiffener theory of [4], which does not consider discreteness of the rings - an effect found earlier to be usually negligible in ring-stiffened shells designed to fail by general instability, see [1], [7]and[10]. The test results in the present test program are compared with "classical" SS3 critical loads, which for ring stiffened shells are identical to SS4 critical loads, as was shown in [5]. Local buckling was predicted by eqs. (1) & (7) of [1] as well as with the analysis of [5] for SS4 boundary conditions.

In [1]and[2] the structural efficiency of ring-stiffened shells was studied, by comparing the stiffened shells with isotropic ones of equivalent weight. Though the calculations were based on a non-conservative criterion, which was shown there to favour the equivalent shells, it was observed that the stiffened shells were always more efficient than the "equivalent" isotropic ones. In [2] it was indicated that for lower values of the area-parameter, ( $A_2/ah$ ), the higher values of structural

efficiency were achieved, in spite of the low values of "linearity" obtained for these shells. Applying the same criterion and Eq.(15) of [1] the structural efficiency is also studied here and it is again observed that stiffened shells are more efficient than the "equivalent" isotropic shells.

The present test program, like the earlier ones [1] & [2] indicates that the dominant stiffener parameter is the area parameter,  $(A_2/ah)$ . For most shells with values of  $(A_2/ah) > 0.3$  buckling loads of 80 percent of those predicted by "classical" linear theory, or higher, were obtained.

## 2. TEST SET-UP AND PROCEDURE

The test set-up for the present test program is shown in Fig. 2. The loading frame is identical to that of [14]. Loading and test procedure, as well as specimen mounting are the same as in [3] (for details see Section 4 and Fig. 4 of [3]).

As in [1], [2], [3] and [14] the specimen are not clamped to the supporting discs. They are just located between the lower disc and an identical top one. The "heavy" end rings of the shell have thin ridges that represent a continuation of the shell. (see Fig. 4 of [1]), to ensure that the load is applied through the shell mid-surface and hence the end moments discussed in [9] to [13] are avoided. The present test boundary conditions are therefore somewhere between SS3 and SS4 boundary conditions (simple supports,

$$w = M_x = 0$$

$$N_x = v = 0 \text{ for SS3, and}$$

$$u = v = 0 \text{ for SS4) and probably never to SS4.}$$

However, it was shown in [5] that for the shell and stiffener geometries of the test specimens geometries, the SS3 and SS4 boundary conditions yield identical critical loads. The restraint to rotation is also not large and its effect for ring stiffened shells under axial compression is negligible anyhow.

About 48 gages were bonded to the surface of each specimen. Six of the gages were located at the mid length of the shell. Their purpose is confirmation of elastic behavior up to buckling and adjustments for uneven distribution of the applied load. The remaining gages were oriented circumferentially and served for detection of local bending. All the gages assisted in detection of incipient buckling, but as in the earlier tests([1], [2], [3] and [14]), it was observed that the circumferential gages are better for this purpose because of their greater sensitivity to bending. Strain gage readings were recorded on a B & F multichannel strain plotter and attempts were made to obtain southwell plots from the strain records (see bibliography in [3] and [14]). For this purpose again the circumferential gages are more effective (see [1] to [3]).

The thickness of the specimens was measured carefully at many points prior to each test. The shell was divided into 12 segments and measurements of every subshell and ring were taken along the meridian lines dividing the shell into segments.

### 3. TEST SPECIMENS

29 integrally ring stiffened shells were tested in the present program. The geometry of the shells is defined in Fig. 1 and their dimensions and geometrical parameters are presented in Table 1.

All the specimens were designed to ensure predomination of general instability and elastic buckling. The specimens were machined from 7075-T6 Aluminium alloy tubes (10" in diameter and 1/2" wall thickness) with mechanical properties, that may be approximated by a Ramberg-Osgood stress-strain relation [15]

$$\epsilon = \sigma/E + K(\sigma/E)^n$$

for which

$$E = 0.75 \times 10^4 \text{ kg/mm}^2 = 1.06 \times 10^7 \text{ p.s.i.}$$

$$\sigma_{0.1\%} = 54 \text{ kg/mm}^2 = 7.67 \times 10^4 \text{ p.s.i.}$$

$$K = 2.4 \times 10^{56}$$

$$n = 28$$

(see also Fig. 5 and Section 3 of [14]).

The machining process is similar to that described in [1], except for the mounting of the blank on the mandrel and releasing of the finished stiffened shell from it, which is described in [14].

The precision of the 7075-T6 specimens did not differ from that obtained for the steel specimens of [1] and [2], though they were machined from a softer material. The machining procedure of the present specimens involved the same methods of cutting and control as in [1] and [2] and hence similar accumulated errors were introduced in the present shells. For the present shells the worst



deviation in shell thickness for a few shells was up to 5% of the minimum skin thickness. The average deviation was, however, within 3% of the minimum thickness.

The aim of the present test program is the study of the effect of stiffener geometry on the "linearity" obtained. Hence the stiffener-parameters:  $(e_2/h)$ ,  $(A_2/ah)$ , and consequently  $(I_{22}/ah^3)$  and  $\eta_{t2}$  were varied. To assure elastic buckling the specimens were designed to fail at stresses less than half the "yield" strength,  $\sigma_{0.1\%}$ , of the shell material.

#### 4. EXPERIMENTAL RESULTS AND DISCUSSION

The experimental buckling loads are given in Table 2. These loads are correlated with the predicted critical loads corresponding to SS3 boundary conditions (see Section 1); or for externally ring stiffened shells, which buckle in an axisymmetric mode (see [4]) with the simple formula

$$P_{GS} = [3(1-\nu^2)]^{-1/2} 2\pi h^2 E [1 + (A_2/ah)]^{1/2} = P_{c1} (\Delta_R)^{1/2}$$

These predictions are also presented in Table 2 as  $(P_{cr})_{SS3}$  and  $(P_{cr})_{App}$  to obtain the "linearity",  $\rho = P_{exp}/P_{cr}$ . The correlation with linear theory, represented by the "linearity"  $\rho$ , is shown in Fig. 3 versus the ring-area parameter,  $(A_2/ah)$ , in Fig. 4 versus the ring spacing  $(a/h)$  and in Fig. 5 versus a combination of these two parameters  $(a/h)[1 + (A_2/ah)]^{-1/2}$ . These figures also include the results of other investigations, [1], [2] and [6] to [8].

Like in [1] and [2], Fig. 3 indicates that the "linearity" is primarily influenced by the area parameter,  $(A_2/ah)$ . It is observed that even for "weak" stiffening represented by low values of the area parameter,  $(A_2/ah) \approx 0.15$ , a reasonably high linearity of 70 percent and above, is obtained. This conclusion is confirmed by the results of the other studies [1], [2] and also [6] to [8], also presented in Fig. 3. It may be noted also that the present results fall within the scatter band of the other studies. Fig. 3 also shows that increasing of area parameter does not improve the "linearity", whereas the weight of the shell increased noticeably. In other words, whereas the gain in "linearity" is only a few percent, the weight of the shell is directly proportional to the increase in the area parameter,

$(A_2/h)$ . Hence, there is a loss in structural efficiency for heavily stiffened shells to be discussed later. Fig. 3 shows that the "linearity" decreases noticeably in the range  $(A_2/ah) < 0.15$  and the values of " $\rho$ " obtained in this range are very similar to those of unstiffened shells. Similar results appear in Fig. 12 of [1] and Fig. 4 of [16] for ring-stiffened conical shells and yielded similar conclusions.

In Fig. 4 the effect of ring spacing  $(a/h)$  on the "linearity" is examined. In spite of considerable scatter a decrease in "linearity" can be discerned in this figure with increase in ring spacing  $(a/h)$ . This influence is apparently contradicted by the results of [8], but it should be noticed that [8] deals with very heavily stiffened shells in comparison with most of the shells studied here and in the other investigations, presented in Fig. 4.

Correlation may be improved, if instead of ring spacing,  $(a/h)$ , the combination  $(a/h)[1 + (A_2/ah)]^{-1/2}$  is considered, as in Fig. 5. Here the trend of decrease in "linearity" with increase of the above mentioned combined parameter is more noticeable. Even the results of [8] almost fall within the scatter band of the present results and the studies of [1], [2] and [6] to [8].

Figs. 3 to 5 indicate that the dominant parameter, for applicability of linear theory is the ring area parameter  $(A_2/ah)$ , and linear theory is even adequate for prediction of buckling loads in relatively "weak" stiffened shells. An area parameter of  $(A_2/ah) \approx 0.15$  represents a lower bound for applicability of linear theory.

The structural efficiency of ring stiffened shells is now studied by Eq. (15) of [1]

$$\eta = \rho \frac{[\Delta_R + (R/100h)]^{1/2}}{(\Delta_R)^2}$$

The results are given in Table 2 and are shown in Fig. 6 versus the area parameter,  $(A_2/ah)$ . Fig. 6 indicates a clear and significant decrease in efficiency with increase of ring area-parameter,  $(A_2/ah)$ . The "equivalent weight" isotropic shell becomes more efficient for relatively low "values" of this parameter,  $(A_2/ah) \approx 0.6$ , in spite of the high "linearity" achieved for these shells. Fig. 6 shows clearly that weakly stiffened shells are more efficient, in spite of their relatively low "linearity". From a design point of view the important point to be noted is that attempts to achieve very high values of "linearity" carry weight penalties which result in an inefficient structure, whereas for low values of the area parameter,  $A_2/ah \approx 0.2$  values of efficiency of 150% or more are obtained. Fig. 3 shows that even for these low values of  $(A_2/ah)$ , a "linearity" of 70 to 90 percent may be obtained. It should be remembered that Eq. (15) of [1] actually favours the equivalent weight isotropic shell, so that in reality the efficiency of the stiffened shells is even higher than that represented in Fig. 6 and Table 2.

In the design of the specimens, the ring-spacing which ensures local "linear" behavior of the subshells was calculated with the criterion for axisymmetric buckling; Eq. (3) of [1]

$$(a/h) < [2.85(1 - \nu^2)^{-1/2} (R/h)]^{1/2}$$

Safe spacings are presented by  $Q$  in Table 2 and a comparison of these  $Q$  with the measured values of  $(a/h)$  in Table 1, shows that all the tested shells fulfill the requirement  $(a/h) < Q$ .

The local critical loads of the subshells were calculated with aid of Eq. (1) of [1]

$$P_{cr} = P_{cl} [1 + (12Z'^2/\pi^4)] / 0.702 Z', \text{ where}$$

$$P_{cl} = [3(1 - \nu^2)]^{-1/2} 2\pi h^2 E$$

and are also given in Table 2 by  $(P_{Loc})_{SS3}$ . For most of the tested specimens these values exceeded those predicted for general instability, except shells AR-4a, AR-4b, AR-7, AR-8b, AR-8c and AR-15 (see Table 2). As mentioned in [1] the critical loads  $(P_{Loc})_{SS3}$  are rather conservative since they correspond to the relatively weak SS3 boundary conditions. Actually the SS4 or some elastically restrained boundary conditions are more applicable to the subshells. Hence, the critical loads for elastically restrained boundary conditions, Eq. (7) of [1].

$$(P_{cr}/Eh^2) = 2\pi \left[ \frac{(n\beta)^2}{12(1-\nu^2)(R/h)} + \frac{(R/h)}{(n\beta)^2} + (k_R/ER^2) (R/h)^2 (R/L) \right] \text{ and}$$

for SS4 boundary conditions were also calculated for these shells and are presented in Table 2 by  $(P_{Loc})_{spring}$  and  $(P_{Loc})_{SS4}$  respectively. These calculations also assure general instability for these shells satisfying the condition for general instability

$$P_{\text{general instability}} < P_{\text{local instability}}$$

Hence, predicted failure by general instability was verified for all the test specimens.

The attempts to apply the modified Southwell method as in [1] to [3],[14] and [16] (see [3] for detailed bibliography) did not yield any meaningful results. The gages bonded to the surface of the shells behaved almost linearly up to buckling and hence practically no data for the Southwell plots could be extracted from the load-strain curves recorded by the gages during the various stages of loading.

Some typical postbuckling patterns are shown in Fig. 7. For the weakly stiffened shells AR-1a and AR-2a the two-tier diamond shape pattern extends over the whole length of the shell. As the stiffening becomes heavier in shells AR-10b and AR-11a, the pattern again has two tiers of diamonds but the diamonds are narrower and do not cover the whole length of the shell. These patterns are similar to those obtained in Fig. 5 of [1].

As discussed in [1], an axisymmetric mode of buckling is expected for externally ring-stiffened shells. No such modes were observed at the tests. However, it seems that a trend towards such an initial mode can be confirmed from the strain records.

As in [1], one notices that the strain gages become "lively" at many locations simultaneously close to buckling. The gages which are located in rows over complete circumferences deviate in each row unidirectionally, indicating axisymmetric deformation. The strain gages readings indicate a complete pattern of incipient buckling covering the whole shell, as assumed by theory and which the usual diamond pattern contradicts. The initiation of an apparently axisymmetrical mode may also be seen in Fig. 8, where it was attempted to photograph this process. Fig. 8 shows the growth of surface deflections of shell AR-14a at stages of loading very close to buckling ( $P = 1900$  kg;  $2000$  kg and  $2100$  kg). In this shell the critical load obtained in the test was  $2200$  kg, exactly as predicted by linear theory. The growth of a periodic and apparently axisymmetric mode along a generator appears very clearly in this figure.

ACKNOWLEDGEMENT

The authors would like to thank the staff and students of the Aircraft Structures Laboratory of the Department of Aeronautical Engineering for their assistance during the course of the tests, to Mmes L. Spector and M. Kuperman for their assistance with the computations and Mr. A. Greenwald for preparing the figures.



REFERENCES

1. Singer, J., "The Influence of Stiffener Geometry and Spacing on the Buckling of Axially Compressed Cylindrical and Conical Shells", Theory of Thin Shells, Proceedings of 2nd UTAM Symposium on Theory of Thin Shells, Copenhagen, September 1967, pp. 234-263, Springer-Verlag, Berlin 1969.
2. Weller, T., "An Experimental and Theoretical Study of Buckling under Axial Compression of Stiffened Cylindrical Shells", D.Sc. Thesis, Technion Israel Institute of Technology, Haifa, Feb. 1971 (in Hebrew).
3. Weller, T., Singer, J., and Nachmani, S., "Recent Experimental Studies on Buckling of Integrally Stiffened Cylindrical Shells under Axial Compression", TAE Report 100, Technion Research and Development Foundation, Haifa, Israel, Feb. 1970.
4. Singer, J., Baruch, M., and Harari, O., "On the Stability of Eccentrically Stiffened Cylindrical Shells under Axial Compression", International Journal of Solids and Structures, Vol. 3, pp. 445-470, 1967. Also TAE Report No. 44 Technion Research and Development Foundation, Haifa, Israel, December 1965.
5. Weller, T., Baruch, M., and Singer, J., "Influence of In-Plane Boundary Conditions on Buckling Under Axial Compression of Ring-Stiffened Cylindrical Shells", Israel Journal of Technology, Vol. 9, No. 4, pp. 397-410, July 1971. Also TAE Report No. 101, Technion Research and Development Foundation, Haifa, Israel, October 1970.

6. Milligan, R., Gerard, G., Lakshminathan, C., and Becker, H.,  
"General Instability of Orthotropic Stiffened Cylinders under Axial Compression", AIAA Journal, Vol. 4, No. 11, pp. 1906-1913, November 1966.
7. Singer, J., Arbocz, J., and Babcock, C.D., "Buckling of Imperfect Stiffened Cylindrical Shells under Axial Compression", AIAA Journal, Vol., 9, No. 1, pp. 68-75, January, 1971.
8. Almroth, B.O., "Influence of Imperfections and Edge Restraint on the Buckling of Axially Compressed Cylinders," NASA CR-432, April 1966. Also presented at the AIAA/ASME 7th Structures and Materials Conference, Cocoa Beach, Florida, April 18-20, 1966.
9. De Luzio, A., Stuhlman, C.E., and Almroth, B.O., "Influence of Stiffener Eccentricity and End Moment on Stability of Cylinders in Compression", AIAA Journal, Vol. 4, No.5, pp. 872-877, May 1966.
10. Block, D.L., "Influence of Discrete Ring Stiffeners and Pre-buckling Deformations on the Buckling of Eccentrically Stiffened Orthotropic Cylinders, NASA TN D-4283, Jan. 1968.
11. Seggelke, P., and Geier B., "Das Beulverhalten versteifter Zylinderschalen", Zeitschrift fuer Flugwissenschaften, Vol. 15, No. 12, 1967, pp. 477-490.
12. Hutchinson, J.W., and Frauenthal, J.C., "Elastic Postbuckling Behavior of Stiffened and Barreled Cylindrical Shells", Journal of Appl. Mech., Vol. 36, Series E, No. 4, pp. 784-790, Dec. 1969.

13. Chang, L.K., and Card, M.F., "Thermal Buckling Analysis for Stiffened Orthotropic Cylindrical Shells", NASA TN D-6332, April 1971.
14. Weller, T., and Singer, J., "Experimental Studies on the Buckling of 7075-T6 Aluminium Alloy Integrally Stringer-Stiffened Shells", TAE Report No. 135, Technion Research and Development Foundation, Haifa, Israel, November, 1971.
15. Ramberg, W., and Osgood, W.R., "Description of Stress-Strain Curves by Three Parameters", NACA Technical Note No. 902, 1943.
16. Weller, T., and Singer, J., "Experimental Studies of Buckling of Ring-Stiffened Conical Shells under Axial Compression", Experimental Mechanics, Vol. 10, No. 11, pp. 449-456, November, 1970.

TABLE 1 - RING STIFFENED SHELLS - DIMENSIONS

Shell	L (mm)	R (mm)	h (mm)	R/h	L/R	Z	d [mm]	c [mm]	a (mm)	$e_2/h$	$A_2/ah$	$I_{22}/ah^3$	$\eta_{t2}$	$Z'$	a/h
AR-1a	108	120.37	.238	506	.897	388.42	.262	.75	6	-1.05	.138	.0139	.1814	1.199	25.21
AR-1b	108	120.37	.244	493	.897	378.87	.252	.75	6	-1.02	.129	.0115	.1513	1.169	24.59
AR-2a	108	120.37	.244	493	.897	378.87	.259	1	6	-1.03	.177	.0166	.2343	1.169	24.59
AR-2b	108	120.37	.239	503	.897	386.79	.262	1	6	-1.05	.183	.0183	.2573	1.19	25.1
AR-3a	108	120.38	.254	474	.897	363.92	.274	.5	6	-1.04	.0899	.0087	.0965	1.12	23.62
AR-3b	108	120.38	.25	482	.897	369.74	.265	.5	6	-1.03	.0883	.0083	.0933	1.142	24.00
AR-4a+	104	120.37	.249	483	.864	344.27	.224	.6	8	-.950	.0675	.0046	.0589	2.352	32.13
AR-4b+	104	120.38	.25	482	.864	342.86	.242	.6	8	-.984	.0726	.0057	.0715	2.347	32.00
AR-5a	105	120.35	.202	596	.872	432.64	.145	1	5	-.1859	.144	.0062	.0946	1.413	29.7
AR-5b	105	120.35	.204	590	.872	428.40	.143	1	5	-.851	.140	.0057	.0871	1.352	28.92
AR-5c	105	120.35	.202	596	.872	432.64	.148	1	5	-.866	.147	.0066	.1005	1.413	29.7
AR-6b	108	120.39	.270	446	.897	342.33	2.29	.6	6	-4.74	.783	4.69	4.53	1.241	24.07
AR-7+	108	120.37	.231	521	.897	400.19	1.78	.6	6	-4.35	.770	3.81	5.50	1.449	28.14
AR-8c+	108	120.36	.221	545	.897	418.33	1.78	.6	6	-4.53	.805	4.35	6.28	1.424	28.51
AR-8a	108	120.37	.236	510	.897	391.71	1.77	.6	6	-4.24	.749	3.50	5.10	1.209	25.42
AR-8b	108	120.37	.243	495	.897	380.43	1.76	.8	6	-4.13	.967	4.24	10.47	1.173	24.69
AR-9a	108	120.38	.263	458	.897	351.47	1.238	.4	6	-2.85	.314	.579	.808	1.085	22.81
AR-9b	108	120.37	.248	485	.897	372.76	1.245	.4	6	-3.01	.335	.703	.969	1.150	24.19
AR-10a	108	120.38	.254	474	.897	363.92	.751	1	6	-1.98	.493	.359	3.26	1.123	23.62
AR-10b	108	120.37	.247	487	.897	374.27	.754	1	6	-2.03	.509	.395	3.58	1.154	24.29
AR-11a	108	120.38	.264	456	.897	350.14	.740	.6	6	-1.90	.280	.184	1.03	1.081	22.73

TABLE 1. - CONTINUED

Shell	L (mm)	R (mm)	h (mm)	R/h	L/R	Z	d [mm]	c [mm]	a (mm)	e <sub>2</sub> /h	A <sub>2</sub> /ah	[ <sub>22</sub> /ah <sup>3</sup>	η <sub>t2</sub>	z'	a/h
AR-11b	108	120.38	.254	474	.897	363.92	.743	.6	6	-1.96	.293	.209	1.17	1.123	24.49
AR-12a	108	120.37	.240	502	.897	385.18	1.26	.8	6	-3.13	.699	1.61	6.60	1.190	25.00
AR-12b	108	120.37	.244	493	.897	378.87	1.266	.8	6	-3.09	.692	1.55	6.31	1.169	24.59
AK-13a	108	120.38	.253	476	.897	365.36	.743	.8	6	-1.97	.392	.281	2.12	1.128	23.72
AR-13b	108	120.38	.254	474	.897	363.92	.743	.8	6	1.96	.390	.278	2.10	1.123	23.62
AR-14a	108	120.37	.247	487	.897	374.27	1.258	.7	6	-3.05	.594	1.28	4.37	1.154	24.29
AR-14b	108	120.38	.253	476	.897	365.36	1.258	.7	6	-2.99	.580	1.20	4.07	1.128	23.72
AR-15	108	120.35	.195	617	.897	474.15	2.274	.5	6	-6.33	.972	11.01	7.70	1.462	30.77

TABLE 2

BUCKLING OF RING-STIFFENED SHELLS - EXPERIMENTAL RESULTS AND COMPARISON WITH LINEAR

THEORY

Shell	$P_{exp}$ [kg]	$(P_{cr})_{App}$ [kg]	$P_{cr}$ SS3 [kg]	n	N	$\rho = \frac{P_{exp}}{P_{cr}}$	$P_{cl}$ [kg]	$(P_{LOC})_{SS3}$ [kg]	$(P_{LOC})_{SS4}$ [kg]	$(P_{LOC})_{"spring"}$ [kg]	Q	$\eta$
AR-1a	1190	1720	1720	12	18	.692	1620	2260		2260	38.88	1.33
AR-1b	1220	1800	1810	12	18	.674	1700	2420		2420	38.38	1.30
AR-2a	1450	1840	1840	12	18	.788	1698	2420		2420	38.38	1.41
AR-2b	1490	1770	1770	12	18	.842	1630	2290		2290	38.77	1.50
AR-3a	1140	1920	1930	12	18	.591	1840	2700		2700	37.63	1.21
AR-3b	1370	1860	1840	12	18	.745	1780	2580		2580	37.95	1.51
AR-4a	1300	1830	1800	11	13	.722	1770	1800*	1970	1870	37.99	1.52
AR-4b	1270	1850	1820	11	13	.694	1780	1810*	1930	1890	37.95	1.45
AR-5a	890	1240	1240	13	21	.718	1160	1460		1890	42.20	1.46
AR-5b	770	1270	1270	13	21	.606	1190	1540		1950	41.98	1.24
AR-5c	750	1250	1250	13	21	.600	1160	1460		1890	42.20	1.21
AR-6b	2710	2780	2780	13	18	.974	2080	2840		3200	36.50	.767
AR-7	1930	2020	2030	14	18	.941	1520	1880*	2110	2090	39.45	.802
AR-8c	1965	1870	1870	14	18	1.05	1390	1740*	1880	1860	40.35	.871
AR-8a	2090	2100	2100	13	18	.995	1590	2210		2220	39.03	.852
AR-8b	2220	2360	2360	14	18	.941	1680	2390*	2420	2410	38.46	.640
AR-9a	2290	2260	2270	12	18	1.01	1970	2960		2970	36.99	1.425
AR-9b	2090	2030	2030	12	18	1.03	1750	2520		2530	38.07	1.439
AR-10a	2250	2250	2250	13	18	1	1840	2700		2710	37.63	1.121

\*  $(P_{LOC})_{SS3} < P_{cr SS3}$

TABLE 2 - CONTINUED

Shell	$P_{exp}$ [kg]	$(P_{cr})_{App}$ [kg]	$P_{cr}$ SS3 [kg]	n	N	$\rho = \frac{P_{exp}}{P_{cr}}$	$P_{cl}$ [kg]	$(P_{LOC})_{SS3}$ [kg]	$(P_{LOC})_{SS4}$ [kg]	$(P_{LOC})$ "spring" [kg]	Q	n
AR-10b	2180	2140	2140	13	18	1.02	1740	2500		2520	38.14	1.134
AR-11a	2020	2250	2260	12	18	.894	1990	3000		3000	36.91	1.524
AR-11b	1950	2090	2090	12	18	.933	1840	2700		2700	37.63	1.37
AR-12a	2130	2140	2150	13	18	.991	1640	2310		2320	38.73	.891
AR-12b	2230	2210	2210	13	18	1.01	1700	2420		2430	38.38	.909
AR-13a	2060	2150	2160	12	18	.954	1830	2670		2630	37.71	1.28
AR-13b	2080	2170	2170	12	18	.959	1840	2700		2700	37.63	1.28
AR-14a	2200	2200	2200	13	18	1	1740	2500		2510	38.14	1
AR-14b	2300	2290	2300	13	18	1	1830	2670		2680	37.71	1.01
AR-15	1320	1520	1520	15	18	.866	1080	1330*	1370	1340	42.93	.734

\* $(P_{LOC})_{SS3} < P_{cr} SS3$

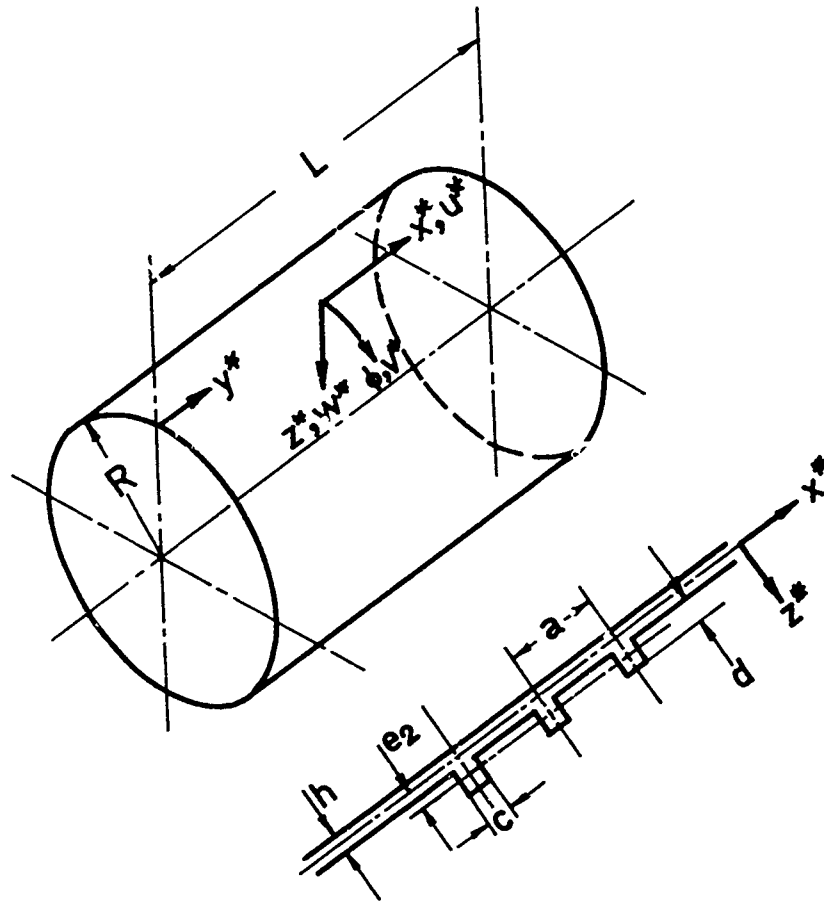


FIG. 1 NOTATION



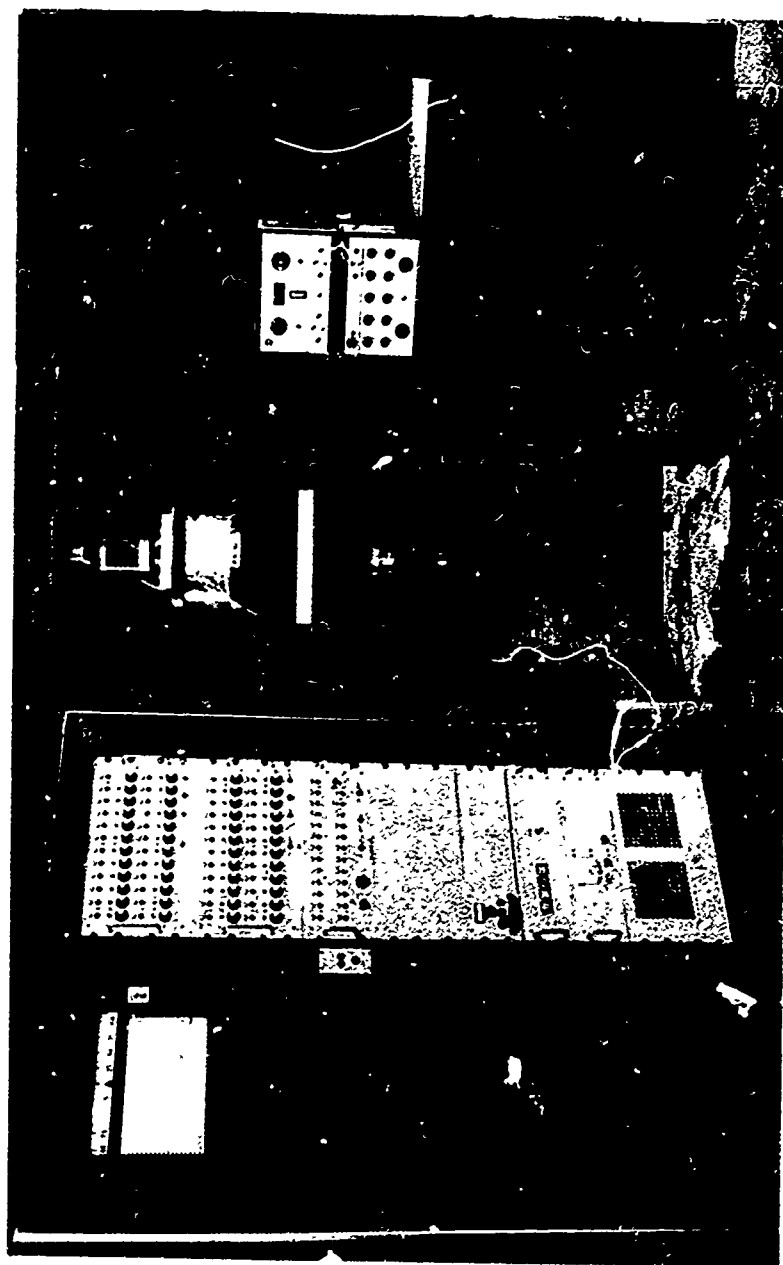


FIG. 2 TEST SET-UP

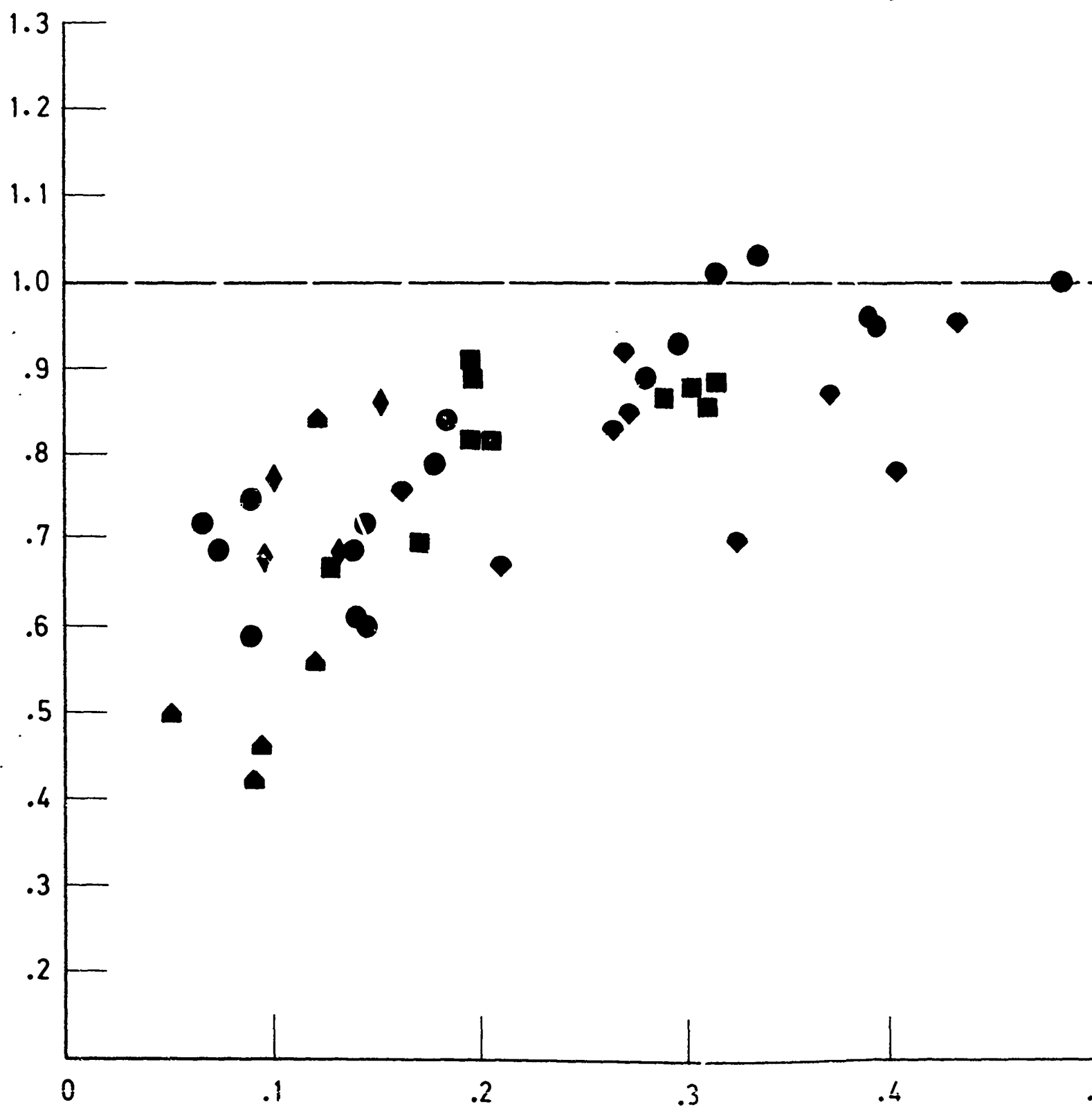
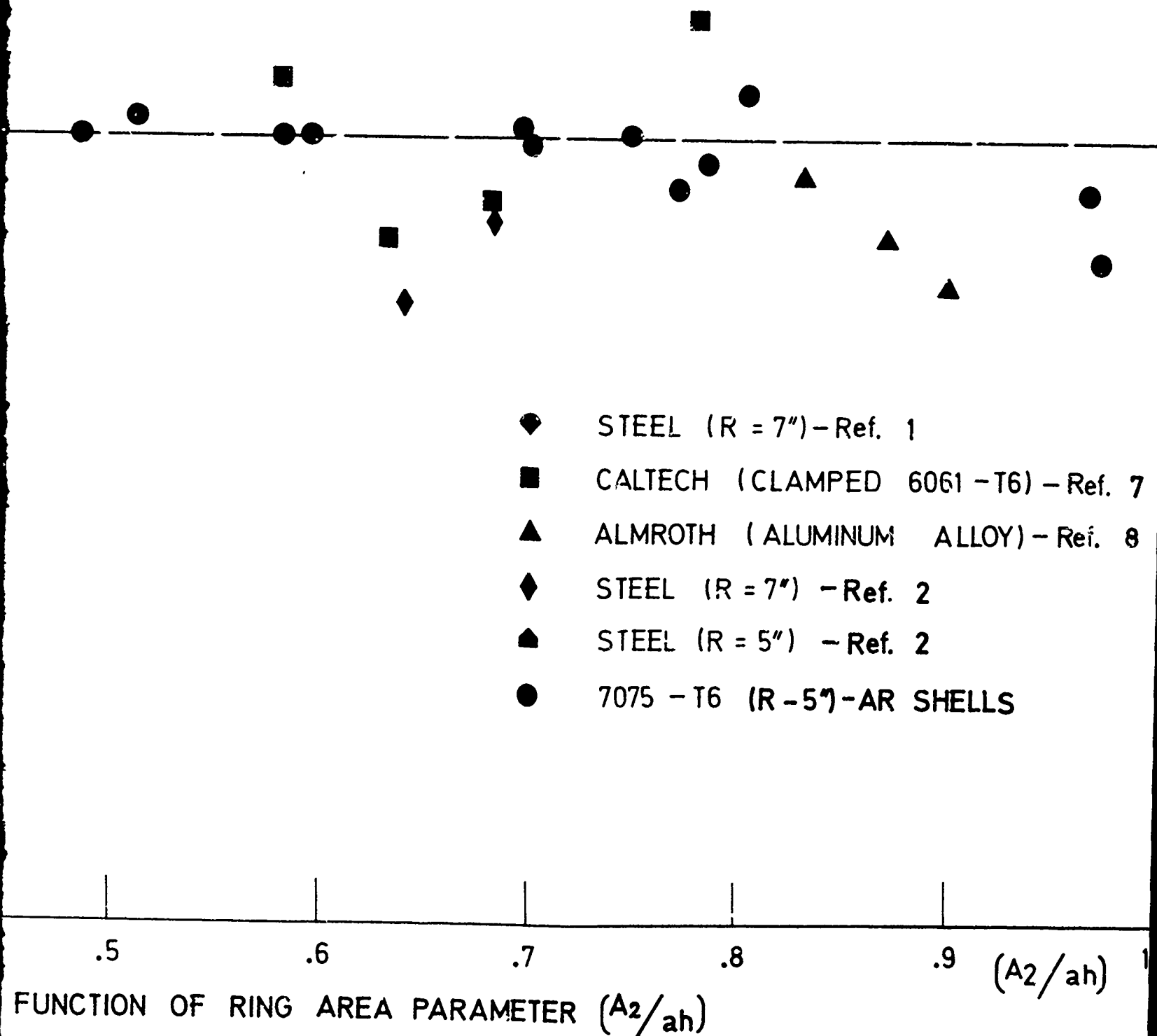
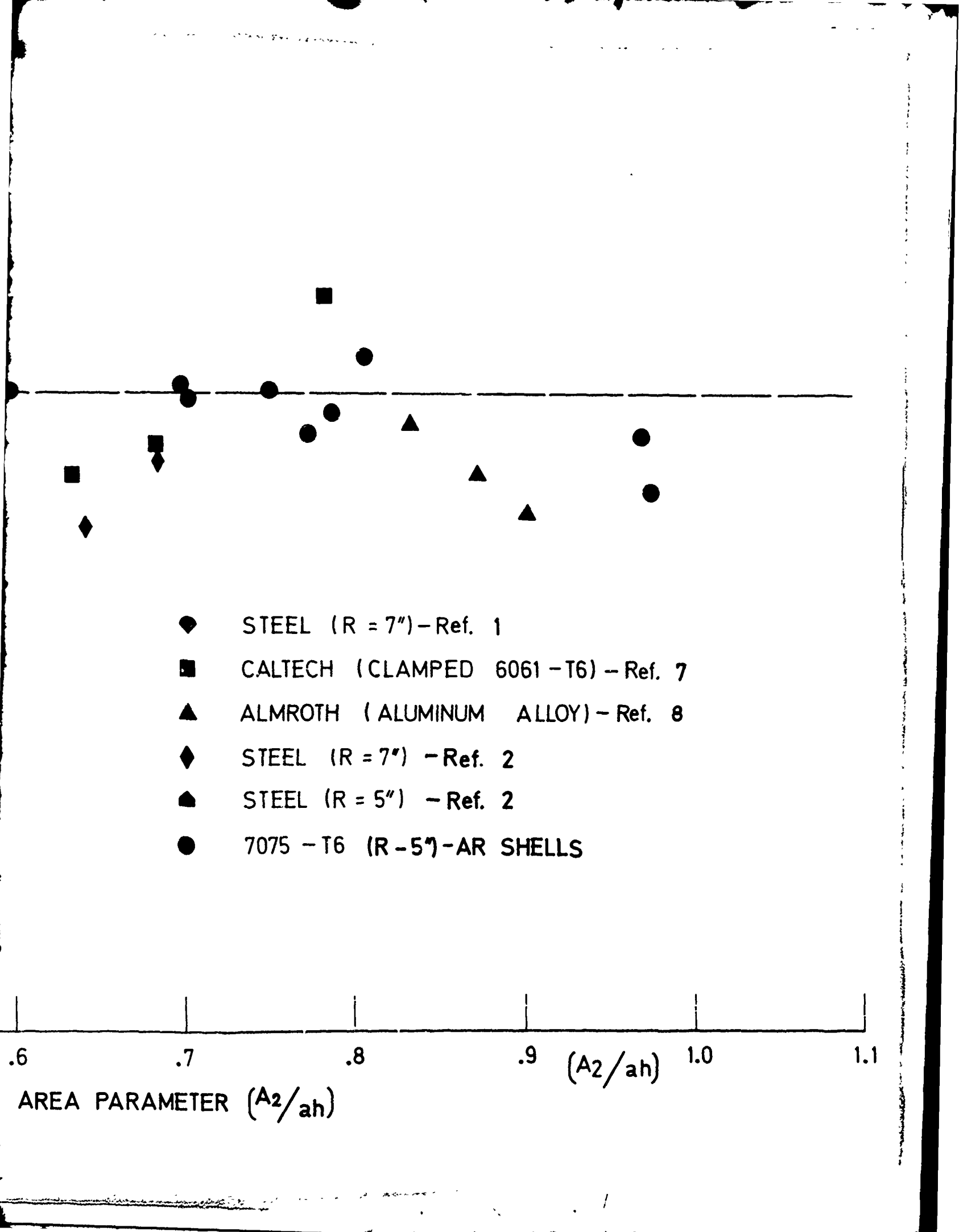


FIG. 3 "LINEARITY" OF RING STIFFENED SHELLS AS A FUNCT



- 
- A scatter plot showing the relationship between the Area Parameter ( $A_2/ah$ ) on the x-axis and various material and reference data points. The x-axis ranges from 0.6 to 1.1 with major ticks every 0.1. A horizontal dashed line is drawn at approximately  $A_2/ah = 0.72$ . Data points are represented by different symbols: diamonds for Steel (R = 7") - Ref. 1, squares for Caltech (Clamped 6061-T6) - Ref. 7, triangles for Almroth (Aluminum Alloy) - Ref. 8, solid diamonds for Steel (R = 7") - Ref. 2, solid triangles for Steel (R = 5") - Ref. 2, and solid circles for 7075-T6 (R = 5")-AR Shells.
- ◆ STEEL (R = 7") - Ref. 1
  - CALTECH (CLAMPED 6061 - T6) - Ref. 7
  - ▲ ALMROTH (ALUMINUM ALLOY) - Ref. 8
  - ◆ STEEL (R = 7") - Ref. 2
  - ▲ STEEL (R = 5") - Ref. 2
  - 7075 - T6 (R = 5") - AR SHELLS

AREA PARAMETER ( $A_2/ah$ )

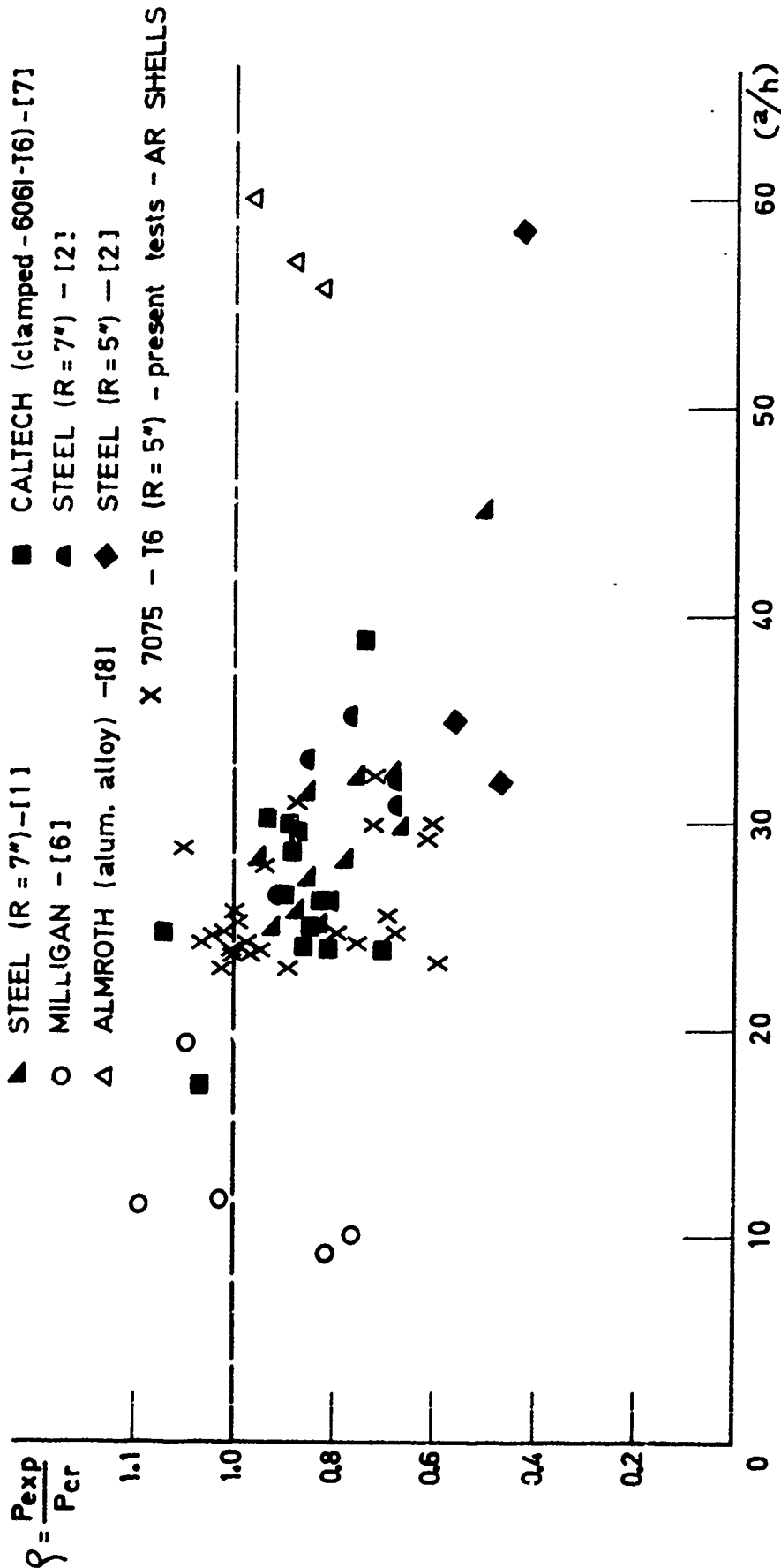


FIG. 4 LINEARITY OF RING-STIFFENED SHELLS AS A FUNCTION OF RING SPACING (a/h)

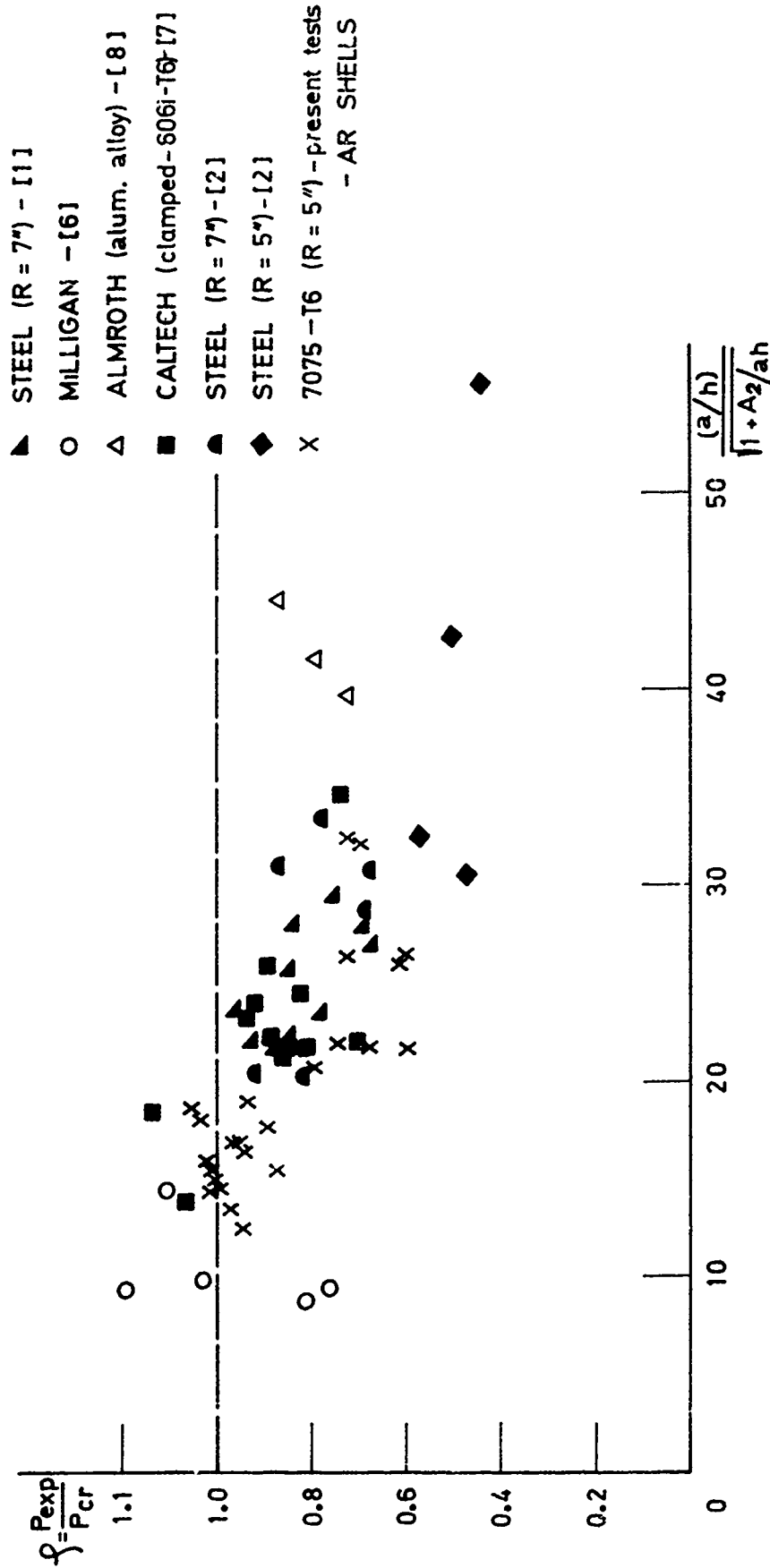


FIG. 5 "LINEARITY" OF RING-STIFFENED SHELLS AS A FUNCTION OF  $(a/h) [1 + (A_2/A_h)]^{1/2}$

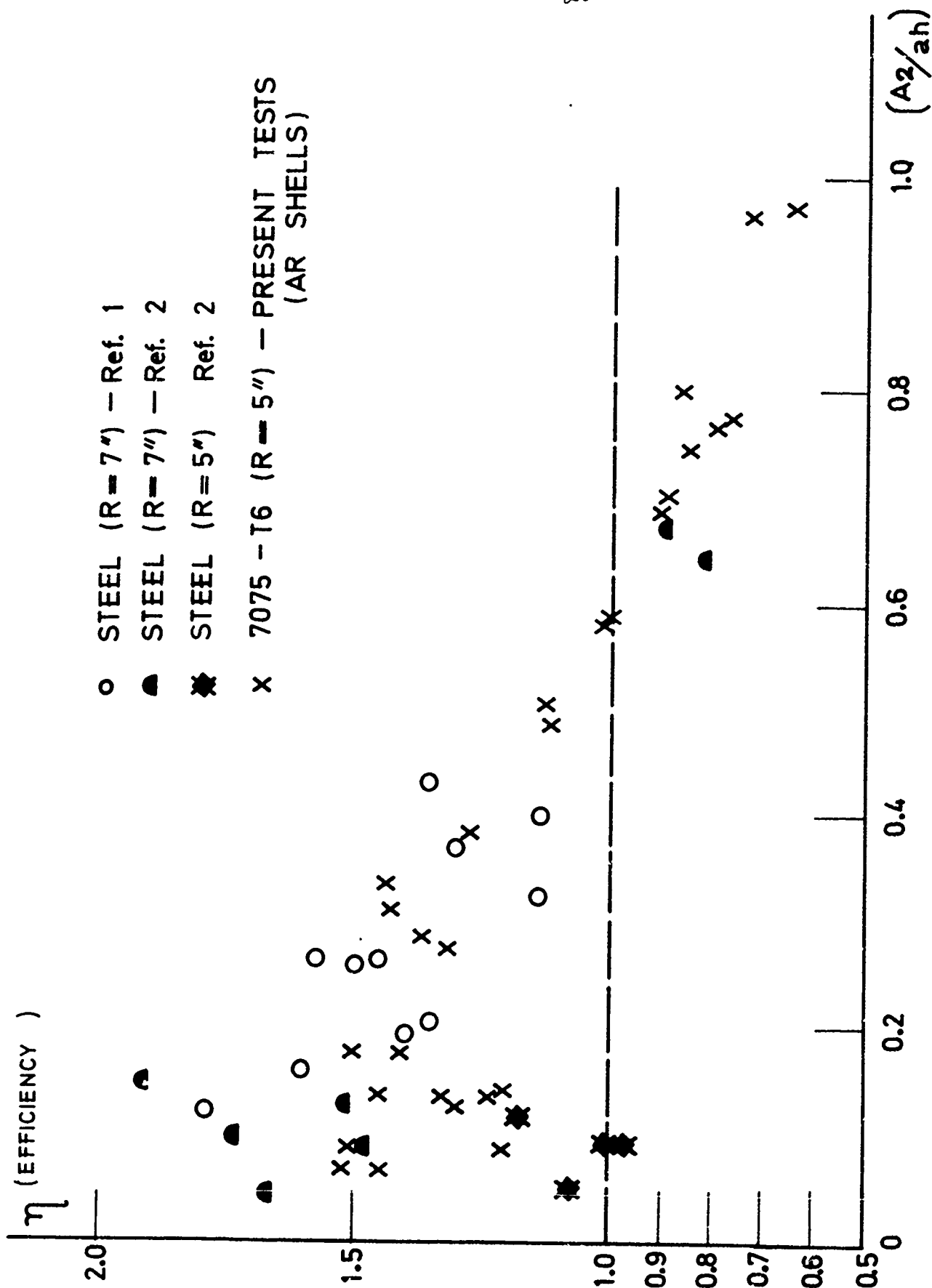


FIG. 6 STRUCTURAL EFFICIENCY OF STIFFENED SHELLS

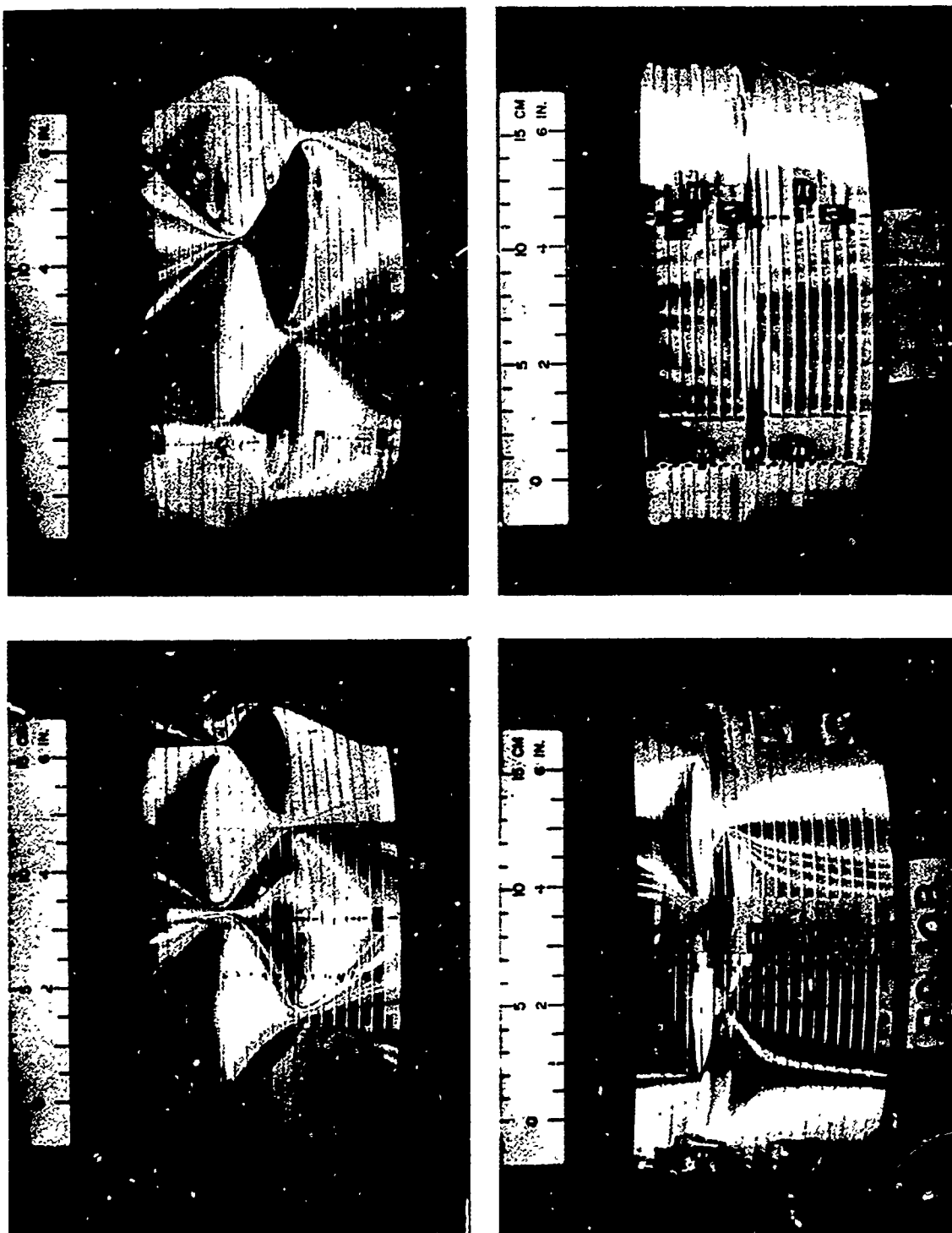


FIG. 7 TYPICAL POST BUCKLING PATTERNS



SHELL AR - 14a

a) 1900 kg

b) 2000 kg

c) 2100 kg

 $P_{exp} = 2200 \text{ kg}$  $P_{cr} = 2200 \text{ kg}$ 

FIG. 8 GROWTH OF SURFACE DEFLECTIONS  
AT STAGES OF LOADING VERY CLOSE  
TO BUCKLING (SHELL AR - 14a)